Characterization and Forecasting of Unstable Resistive Wall Modes in NSTX and NSTX-U*

J.W. Berkery[1], S.A. Sabbagh[1], Y.S. Park[1], R.E. Bell[2], S.P. Gerhardt[2], C.E. Myers[2]

[1]Department of Applied Physics, Columbia University, New York, NY, USA

[2]Princeton Plasma Physics Laboratory, Princeton University, Princeton, NJ, USA

E-mail contact of main author: jberkery@pppl.gov

Abstract. The new Disruption Event Characterization and Forecasting (DECAF) code has been written to analyze disruptions in tokamaks. A quantitative statistical characterization of the chains of events which most often lead to disruption in a database of discharges from NSTX which disrupted due to an unstable resistive wall mode (RWM) is presented. The recently implemented reduced kinetic model for RWM stability is described and shown to have the potential to track RWM stability in real-time for disruption avoidance. The reduced model was tested on a database of discharges from NSTX and experimentally stable and unstable discharges were separated noticeably on a stability map in ExB frequency, collisionality space. Initial results show the reduced model only failed to predict an unstable RWM in 15.6% of cases with an experimentally unstable RWM and performed well on predicting stability for experimentally stable discharges as well.

1. Introduction

Tokamak plasma confinement devices utilize magnetic fields, partially created by a large toroidal plasma current, to contain high pressure plasmas for fusion energy. If the current is disrupted, a loss of plasma confinement can lead to large heat deposition and forces on the surrounding structures. These “disruptions” must be avoided for the safe operation of future devices. To gain understanding needed for this avoidance, first it is important to identify the specific physics elements which comprise disruption event chains. Second, if the events in the disruption chains can be forecast, cues can be provided to an avoidance system to attempt to break the chain. Finally, if avoidance is deemed untenable a mitigation system can significantly reduce disruption ramifications.

In the present work, we describe a new Disruption Event Characterization and Forecasting (DECAF) code which utilizes the comprehensive framework described above. The approach of the code is briefly described in section 2. The ultimate goal is to provide forecasts which integrate with a disruption avoidance system and are utilized in real-time during a device's operation. In the present work we focus in section 3 on quantitative statistical characterization of the chains of events which most often lead to disruption of discharges from NSTX which disrupted due to an unstable resistive wall mode (RWM). Finally, in section 4, we discuss the

*Supported by US DOE Contracts DE-FG02-99ER54524 and DE-AC02-09CH11466.

recently implemented reduced kinetic model for predicting the growth rate of the RWM and apply it a database of NSTX discharges in section 5.

2. The Disruption Event Characterization and Forecasting (DECAF) Code

The DECAF code has been written to analyze disruptions in tokamaks. The code is specifically meant to be portable, in that it was written to easily allow reading data from various machines without changes to source code, and modular, in that the pieces of code related to disruption events and physics models are separated into modules for ease of parallel development of code. The grouping of the physical event modules in DECAF is an automated approach analogous to deVries et al. [1] and the approach to warning algorithms in DECAF follows Gerhardt et al. [2], with each approach being expanded in the present implementation.

The physical event modules of the DECAF code are broken down into individual events. For each event, various tests are performed to determine whether that event has occurred within the discharge. For each discharge, the code finds the chain of events leading up to that disruption by applying one or more warning tests for each of the presently implemented events. At the moment, each of these tests is a simple threshold test, such as the test for excessive pressure peaking which very simply compares the equilibrium reconstruction of the pressure peaking factor ($p_0/\langle p \rangle$) to user-defined thresholds and when $p_0/\langle p \rangle$ reaches each of those levels warning points are issued. When the warning level reaches the point threshold for the event to be declared, the event PRP is declared to have occurred.

Each quantity used in DECAF tests is either directly measured in NSTX, or obtained through equilibrium reconstruction via the NSTX implementation of the EFIT code [3] using magnetics, a diamagnetic loop measurement, and Thomson scattering profiles of the electron density and temperature to partially constrain the pressure profile. In the future, when the analysis is connected to a disruption avoidance system, only causal tests from real-time measurements and real-time equilibrium reconstruction quantities can be used. However, for the purpose of the present analysis, characterizing the disruptions of an existing database of discharges, post-processed quantities will be used.

3. Characterization of a Set of Resistive Wall Mode Disruptions in NSTX

In order to test the code's robustness and gain physics insight, DECAF analysis was performed on a database of 44 NSTX discharges that were pre-determined to have unstable resistive wall modes which lead to disruptions. Resistive wall mode [4] (RWM) is the name given to a tokamak eigenmode which grows on the time scale of the penetration of the field into the surrounding wall structure, τ_w. An unstable, growing RWM can be detected by examining when an exponential growth in the signal on low frequency poloidal magnetic sensors located between the plasma and the vacuum vessel exceeds a pre-set threshold, as is presently implemented in DECAF. In section 4, a more sophisticated kinetic model will be described.

The range of flat-top β_N for the 44 discharges analyzed here was roughly 4-6.5, although it should be noted that β_N has been shown to not be a good predictor of disruptivity by itself [5]. Many of these discharges also had $n = 3$ magnetic braking applied, which slowed the toroidal plasma rotation [6]. Tearing modes were stable during these discharges and therefore no tests for tearing modes will be included in the analysis presented here.

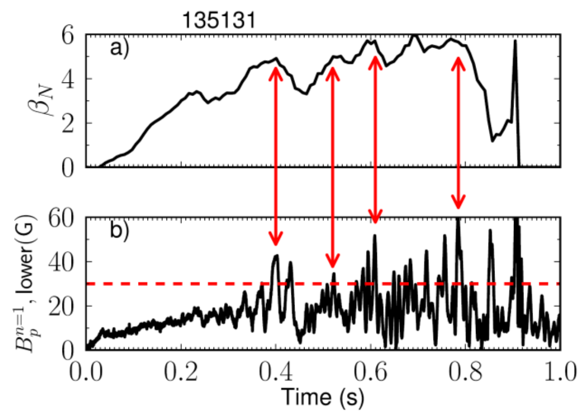

FIG. 1: β_N and n=1 signal on lower poloidal magnetic sensors from NSTX discharge 135131, showing that RWM warnings sometimes indicate minor disruptions that cause decreases in β_N, with subsequent recovery.

The present version of the DECAF code, with eight event tests, was run on the 44 selected discharges to gain insight into common event chains that result during RWM disruptions in NSTX. Naturally, the RWM event was detected in all of the discharges, as were plasma current not meeting request (IPR) and the disruption itself (DIS), by definition. Additionally, loss of wall proximity control (WPC) and low edge safety factor (LOQ) warnings also resulted in each discharge. The pressure peaking warning (PRP) occurred on a majority of the discharges analyzed (34 of 44), but typically occurred with or after the RWM, not before. Loss of vertical stability control (VSC) was present in most of the discharges as well (31 out of 44). Low density (LON) warnings occurred less often in this database (11 out of 44).

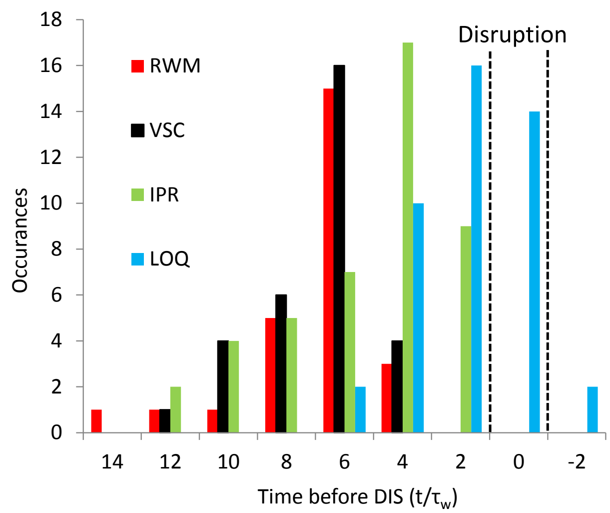

FIG. 2: Histogram of the timing of various disruption chain events in the 44 discharge NSTX database before the time of disruption, within 14 wall times.

With the RWM $B_p^{n=1}$ lower sensor amplitude threshold of 30G ($\delta B/B_0$ ~ 0.67%) used here the RWM warning was typically found near the disruption limit. In 59% of the cases, the RWM event occurred within 20 τ_w of the time of disruption (DIS) (τ_w is the time scale of penetration of magnetic flux through the conducting structure, taken here to be 5 ms). Additionally, many of the earlier RWM warnings could not be considered false positives; they cause significant thermal collapses or "minor disruptions", with subsequent recovery (as illustrated in Fig. 1).

One way of seeing which events are commonly associated is to examine a histogram of some of the timing of the events before the time of disruption (DIS), shown in Fig. 2. Here only the events within 14 τ_w of the disruption are shown, where τ_w is taken to be 5 ms; there are some RWM events at earlier times which are not shown here. It is clear that LOQ and IPR events occur close to the time of disruption, and these are often preceded by VSC, and RWM events which peak around 30 ms prior to the disruption.

Event chain	Percent
RWM $\rightarrow$ VSC $\rightarrow$ PRP	15.9%
RWM $\rightarrow$ WPC $\rightarrow$ PRP	13.6%
RWM $\rightarrow$ IPR $\rightarrow$ WPC	11.4%
RWM $\rightarrow$ PRP $\rightarrow$ IPR	11.4%
RWM $\rightarrow$ WPC $\rightarrow$ VSC	9.1%
RWM $\rightarrow$ VSC $\rightarrow$ WPC	9.1%

TABLE 1: The six most common two-event combinations that directly followed an RWM event in the 44 discharge NSTX database.

Examining the common chain of events more closely can provide insight into how to cue avoidance systems to return to normal plasma operations. The 44 RWMs were followed immediately by WPC and VSC (two events related to plasma motion) each 13 times, PRP 11 times, IPR 6 times, and LOQ once. The RWM event never proceeded to LON or DIS without another event happening first. Considering the two-event chains that happened directly after RWMs, we find that although there are 42 two-event combinations that could occur from the 7 currently tested for (in addition to RWM), six two-event chains accounted for 70% of the cases in this database (table 1).

4. Reduced Kinetic Stability Model Implementation in DECAF

It was previously recognized that simplified model calculations based on physics insight from kinetic stability theory should be examined [5,7]. Now implemented in DECAF is a model based upon simplification of kinetic stability theory [8,9] with collisionality [10], implemented in the RWM dispersion relation: $\gamma\tau_w = \mathrm{Re}[-(\delta W_\infty + \delta W_K)/(\delta W_b+\delta W_K)]$.

Models for ideal fluid stability δW terms have been previously developed for NSTX [7], and have now been implemented in DECAF and tested for NSTX-U discharges. For resistive wall mode (RWM) stability, once the kinetic term δW_K is defined, the normalized growth rate $\gamma\tau_w$ can be calculated from the RWM dispersion relation. For the kinetic δW_K term, full calculations with codes such as MISK [11] cannot be performed in real time. Kinetic RWM stability theory has been developed to greater complexity in recent years, but here we wish to go in the *opposite* direction and simplify kinetic theory to facilitate real-time calculation.

For the present purposes we wish to construct a functional form for δW_K that is easily, quickly calculable and that relies on a few important, measurable parameters. Any such model must capture the essential physics learned from the successful application of kinetic theory to experimental results in recent years. Namely, resonance between ExB frequency, ω_E, and precession drift frequency, ω_D, of trapped thermal ions at lower plasma rotation, and with bounce frequency, ω_b, at higher plasma rotation provides a stabilizing component to δW_K, but in between these the kinetic effects are weaker, allowing for instability [12]. Increased collisionality tends to damp the rotational resonance stabilization (see Fig. 3 of Ref. [10]) and shift it to slightly lower rotation (see Fig. 6 of Ref. [12]). The imaginary terms of δW_K tend to peak at lower plasma rotation than the real parts (see Fig. 8 of Ref. [13]) so that plasmas move in kinetic stability space as rotation changes in looping paths (see Fig. 5 of Ref. [12]).

To that end, Gaussian functions were used to represent kinetic resonances (Fig. 3). The positions of the peaks in <ω_E> are determined by typical experimental ranges of ω_D and ω_b and the height, width, and position all dependent on <ν>. In the following <ω_E> and <ν> represent average values for ExB frequency and collisionality as described in Ref. [5]. The bounce resonance contribution was allowed to continue to increase at high <ω_E> to capture the many bounce harmonics and circulating particle contributions. Coefficients for the functions were selected to reflect NSTX experience.

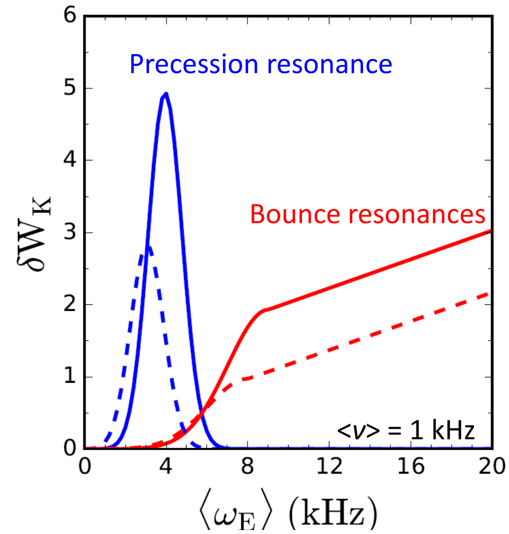

FIG. 3: Modeled real (solid) and imaginary (dashed) δW_K terms for precession (blue) and bounce (red) resonances for NSTX at <ν> = 1 kHz.

Recently, the DECAF code has been expanded to include the necessary measured and derived profiles for the reduced kinetic stability model. This is a significant update to DECAF, as previously it had only dealt with scalar quantities as a function of time. Profiles now included are electron temperature and density profiles from Thomson scattering measurements, ion temperature and density, and carbon ion rotation (ω_φ^C) profiles from charge exchange recombination spectroscopy. From these we derive the ion collision frequency profile and the carbon ion diamagnetic frequency, ω^{*C}. The ExB frequency is obtained via a carbon ion radial force balance from $\omega_E = \omega_\varphi^C - \omega^{*C}$.

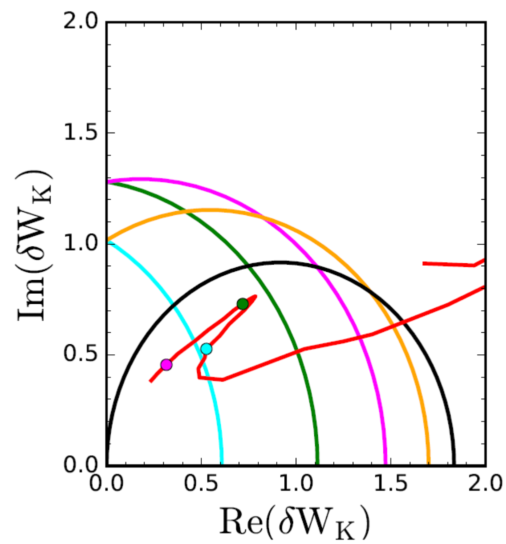

FIG. 4: Trajectory of NSTX discharge 139514 through Re(δW_K) vs Im(δW_K) space. The colored circles indicate the unstable region with increasing C_β.

Once the form of δW_K versus these quantities is established in the model, it is left to implement the model by following the evolution of a plasma discharge in time through the space of these quantities. The procedure is simply laid out as such: 1) Internal inductance, pressure peaking, and aspect ratio are used in the ideal beta limit model to calculate $\beta_{N,no\text{-}wall}$ and $\beta_{N,with\text{-}wall}$ [7]. 2) The ideal β limits and the measured β_N give $C_\beta \equiv (\beta_N - \beta_{N,no\text{-}wall}) / (\beta_{N,with\text{-}wall} - \beta_{N,no\text{-}wall})$. 3) Expressions for the fluid δW terms as functions of C_β that mimic DCON results give δW_b and δW_∞. 4) The ideal δW terms give the fluid growth rate, $\gamma_f\tau_w$, and also set the unstable region in a Im(δW_K) vs. Re(δW_K) stability diagram. 5) Calculated <ω_E> and <ν> are used in the reduced kinetic model to calculate δW_K. 6) Finally, δW_K is used in the kinetic RWM dispersion relation to find $\gamma\tau_w$.

Through the changing levels of total (precession plus bounce terms) real and imaginary δW_K, one can plot the trajectory of the plasma in $Re(\delta W_K)$ vs. $Im(\delta W_K)$ space. This is shown in Fig. 4 along with the unstable regions for various levels of C_β (0.2-1.0). The circular lines indicating the unstable boundary correspond to $\gamma\tau_w = 0$. Inside these circles $\gamma\tau_w$ is positive, and therefore the RWM is unstable. As the plasma moves in time in the δW_K space, at the same time the size of the unstable region is changing as well. Within the plasma trajectory shown, colored circular markers indicate the times that the plasma crosses the corresponding C_β level. So, for example, in this case at the time in the discharge when $C_\beta = 0.2$ (cyan) the plasma is just outside the unstable region while by the time of $C_\beta = 0.4$ (green) and $C_\beta = 0.6$ (magenta) δW_K has decreased due to the changing $<\omega_E>$ and $<\nu>$ and additionally the unstable region has increased in size due to the fluid terms at the larger C_β. The combined effect is that the plasma is now inside the unstable region.

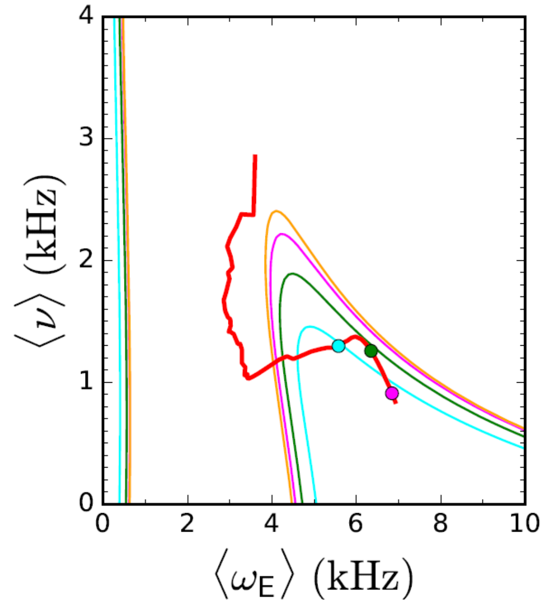

FIG. 5: Trajectory of NSTX discharge 139514 through $<\omega_E>$ vs. $<\nu>$ space. The colored contours represent the unstable region for various levels of C_β.

Alternatively, one can show a stability diagram in the $<\omega_E>$, $<\nu>$ space at a given level of C_β by plotting contours of $\gamma\tau_w$ (similar to Fig. 6 in Ref. [12]). Here we show the trajectory of the same plasma in this space as time increases, $<\omega_E>$ increases, and $<\nu>$ decreases (Fig. 5). Similarly to Fig. 4, in this diagram the unstable region changes with time as C_β changes.

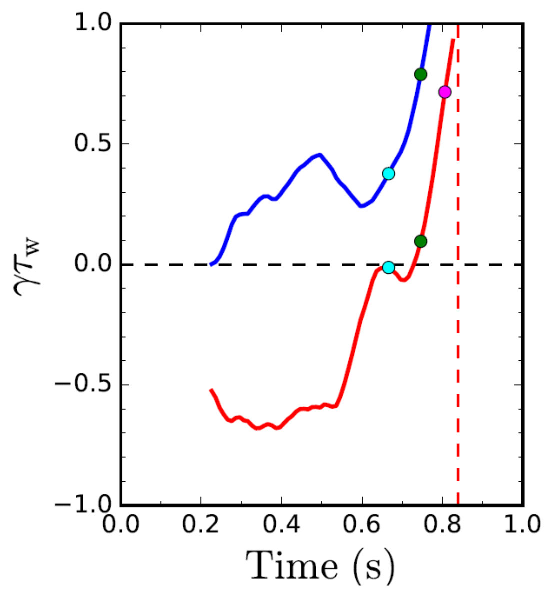

FIG. 6: Calculated ideal (blue) and kinetic (red) normalized growth rates for NSTX shot 139514.

Finally it is natural to simply plot the growth rate vs. time. In Fig. 6 we do this for the same discharge for both the fluid and kinetic growth rate, where it is easy to see the transition into the unstable range at a time of around 0.75s.

5. Application of the Model to an NSTX Database

It is useful now to apply the reduced model to a database of NSTX RWM discharges. For a large number of discharges we will presently show their trajectories on a stability map as in Fig. 5. Also it is natural to simply plot the forecast RWM growth rate as a function of time. Here we plot $\gamma\tau_w$ vs. time before DIS, the time of disruption (as determined by tests within

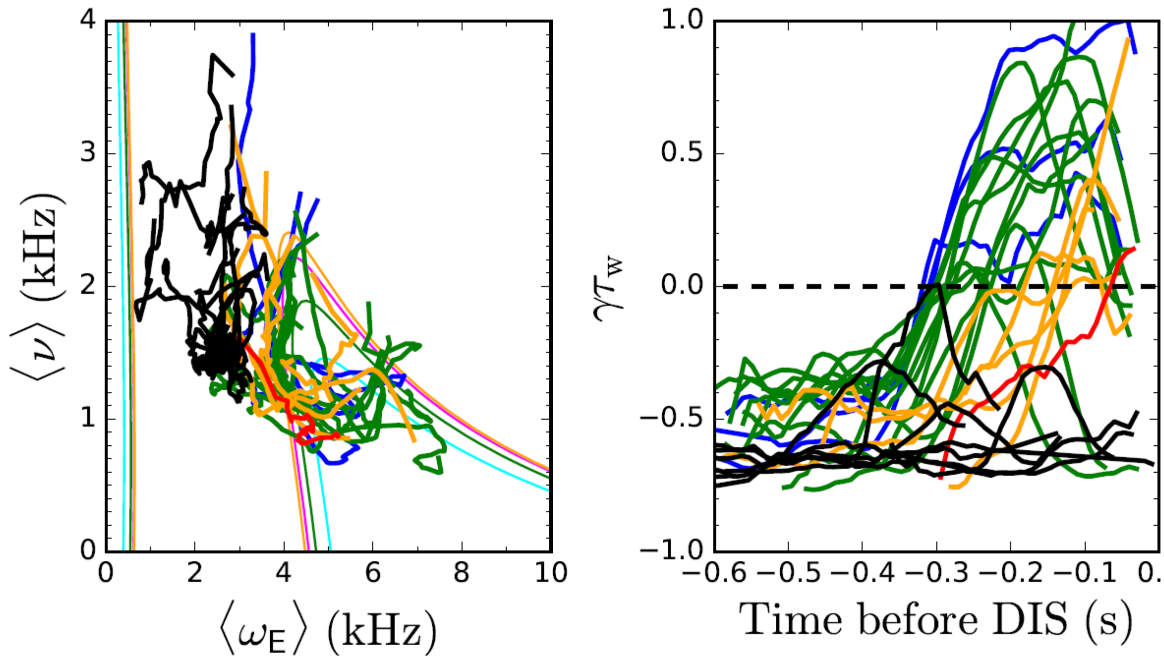

FIG. 7: Stability diagram (left) and forecast growth rate (right) for unstable (colored) and stable (black) NSTX discharges.

DECAF). For discharges without an RWM induced disruption, the time DIS effectively indicates the natural end time of the discharge by other means.

These plots are shown in Fig. 7 for 20 discharges with unstable RWMs in NSTX (color) and 8 without (black). Unstable RWMs were determined to have occurred in these discharges by both independent assessment of relevant signals as well as a threshold test on a poloidal magnetic signal within DECAF. The colors indicate the warning time before disruption when the model indicates the RWM should be unstable ($\gamma\tau_w$ crosses zero). Red is for a single case of < 0.1s warning, orange five cases with 0.1-0.2s, green eleven cases with 0.2-0.3s and blue three cases with 0.3-0.32s warning.

One can see quite clearly a difference in the evolution in $\langle\omega_E\rangle$ vs. $\langle\nu\rangle$ space between the stable and unstable discharges. While all the discharges drop in collisionality with time during the shot, due to increasing temperature, in the unstable cases a turn towards higher $\langle\omega_E\rangle$ leads into the unstable region. This is avoided in all the stable cases shown here (in fact, some drop towards zero $\langle\omega_E\rangle$ leading one case to just barely touch $\gamma\tau_w = 0$).

In addition to the cases shown in Fig. 7, many others were analyzed. In fifteen additional RWM unstable cases, the model also showed $\gamma\tau_w$ crossing zero into the unstable region, but in these cases this occurred well before the disruption and in fact were all correlated with *minor* disruptions that occurred earlier in those shots. Here a minor disruption is defined as a 10% drop in both β_N and stored energy within 0.1s, that subsequently recovers. In each of the fifteen cases considered, $\gamma\tau_w$ crossed zero within 0.1s of a minor disruption. There were, however, other minor disruptions in the database that did not correlate with the reduced kinetic model warning; whether these are due to other causes will be further explored.

In any case, there were 35 discharges in the database where the RWM became unstable leading to a disruption in which the reduced kinetic model predicted instability within 0.32s of the disruption or 0.1s of an earlier minor disruption. Additionally in three experimentally RWM unstable cases, the model gave a warning 0.4s in advance without any related minor disruption, which we consider a false positive because it is so early. Finally, this initial model sometimes misses unstable RWMs. There was one case in which $\gamma\tau_w$ barely didn't cross zero, three cases with very low C_β disruptions that the model missed, and three cases where $\langle\omega_E\rangle$ was in what the model considered to be a stable range, yet an unstable RWM occurred. Altogether the model failed to predict an unstable RWM at all in 7 out of 45 experimentally unstable cases, or 15.6%. The success rate of the model is surprisingly high given its initial state and relative simplicity. Further research will aim to improve the success rate.

Finally, in addition to the eight successful predictions of stability for the experimentally *stable* discharges shown above, five more stable discharges were tested. In three of these cases the discharge evolution in $\langle\omega_E\rangle$ vs. $\langle\nu\rangle$ space was very similar to the *unstable* cases shown in Fig. 7, but nevertheless the discharge remained stable. It is possible that in these cases some other stabilizing effect not captured by the reduced model was present, but this remains to be determined. In two other experimentally stable cases, the RWM warning was triggered by the reduced model because $\langle\omega_E\rangle$ went to zero (hints of this behavior also appear in some of the shots in Fig. 7). The unstable region at $\langle\omega_E\rangle \sim 0$ is present in the model due to theory expectation, but has not yet usefully captured an unstable RWM in our NSTX analysis. This region could be eliminated in the model since we are interested in improving the model's usefulness whether or not it agrees perfectly with theory, but this requires further investigation. If those cases were eliminated then 10 out of 13, or 77%, of stable high β, long-pulse NSTX discharges analyzed were predicted stable in the reduced model.

References

[1] de VRIES, P.C., et al., Nuclear Fusion **51** (2011) 053018.

[2] GERHARDT, S.P., et al., Nuclear Fusion **53** (2013) 063021.

[3] SABBAGH, S.A., et al., Nuclear Fusion **41** (2001) 1601.

[4] CHU, M.S., et al., Plasma Physics and Controlled Fusion **52** (2010) 123001.

[5] BERKERY, J.W., et al., Physics of Plasmas **21** (2014) 056112.

[6] ZHU, W., et al., Physical Review Letters **96** (2006) 225002.

[7] BERKERY, J.W., et al., Nuclear Fusion **55** (2015) 123007.

[8] LIU, Y.Q., et al., Physics of Plasmas **15** (2008) 112503.

[9] BERKERY, J.W., et al., Physics of Plasmas **18** (2011) 072501.

[10] BERKERY, J.W., et al., Physical Review Letters **106** (2011) 075004.

[11] HU, B., et al., Physics of Plasmas **12** (2005) 057301.

[12] BERKERY, J.W., et al., Physical Review Letters **104** (2010) 035003.

[13] BERKERY, J.W., et al., Physics of Plasmas **17** (2010) 082504.